Nordic Hydrology 11, 1980, 187-208

Parametrization of Contaminant Transport through an Anisotropic Unconfined Aquifer

A.G. Bobba and R.P. Bukata
Canada Centre for Inland Waters, Burlington, Ont.

A duo two-dimensional deterministic model of contaminant transport through a homogeneous and anisotropic unconfined aquifer is developed. This model is then utilized to evaluate the effects of such hydrogeologic parameters as convection, dispersion, and chemical adsorption on the build-up, steady-state, and recovery phases of the subsurface contaminant transport. Figures are presented illustrating the dependence of the subsurface transport upon principal velocity ratios, dispersivity ratios, and the adsorption coefficient. The results clearly indicate a distinct dominance of the principal velocity ratio (i.e., degree of aquifer anisotropy) on the transport of subsurface contaminants.

Introduction

Aquifers, being saturated sub-surface zones, play integral roles in the transport of groundwater throughout a basin network. In most basins developed for land-use, such aquifers are relatively close to the surface (the water table generally being considered as the shallowest depth at which the aquifer may be defined) and as such are particularly vulnerable to contamination from such activities as farming and disposal of wastes from industrial sites, in addition, of course, to displaying vulnerability to contaminated precipitation impinging from above. The presence of contaminant concentrations in the saturated zone will greatly impact the

groundwater flow system and may ultimately present hazards to the regional water supply. Contaminants may intrude upon an aquifer either directly through solid waste burial at the water table, or indirectly through seepage from liquid and solid waste storage on the ground surface. This contaminant transport will depend upon such parameters as the hydrogeological nature of the aquifer, the physiochemical properties of the contaminant and saturated zone, and the regional climate.

In recent years, great emphasis has been placed upon numerical solutions of the convective/dispersive transport equations in an attempt to predict the intricacies of groundwater motion. Such predictions, based upon suitable representations of groundwater flow systems, may provide considerable assistance in establishing both the location and the operational practices of waste disposal sites.

Numerous attempts have been made to quantitatively describe the behaviour of contaminants in an aquifer. Most mathematical models have been concerned with simplified one-dimensional convection/diffusion through a soil column (Lapidus et al. 1952) or one-dimensional transport with suitable modifications to include the effects of contaminant adsorption (Kay et al. 1967; Marino, 1974). Two-dimensional solutions to the convection/dispersion transport equation have been recently considered by Bredehoeft et al (1973) and van Genuchten et al. (1977). Most transport models consider the sole phenomenon responsible for groundwater chemical interaction to be adsorption. Such a consideration is, of course, eminently sensible since the fate of any contaminant recharged into the saturated zone is largely dependent upon the capacity of the solid matrix material to adsorb the contaminant and much work has been presented dealing with such adsorption (Banks et al. 1964; Lindstrom et al. 1973). However, the pathways of groundwater flow are determined, in part, by parameters other than adsorption. Such parameters as groundwater velocity, recharge velocity, mineralogical composition of the aquifer, and the chemical reaction coefficient between the solid matrix and the contamination concentration also play important roles in delineating the ultimate impact of contaminants injected into a groundwater flow system.

It is the purpose of this paper to discuss the development of a duo two-dimensional deterministic model of contaminant transport within an unconfined aquifer. The transport model is then used to evaluate the effects of hydrogeologic parameters such as convection, dispersion, groundwater velocity, chemical adsorption, and spatial variation of contaminants on the patterns of groundwater contamination. This paper, the first in an intended series, will follow the bulk of the current hydrological modelling work and consider the unconfined aquifer as being defined by a horizontal (in the local earth system) water table. Clearly, such a model suffers from an obvious departure from reality since the topography of the basin greatly impacts the preferential directions of groundwater flow. Subsequent communications will deal with modeling work currently in progress which considers a three-dimensional water table and the ultimate interaction between the groundwater flow and small lakes located within such a topographically-structured basin.

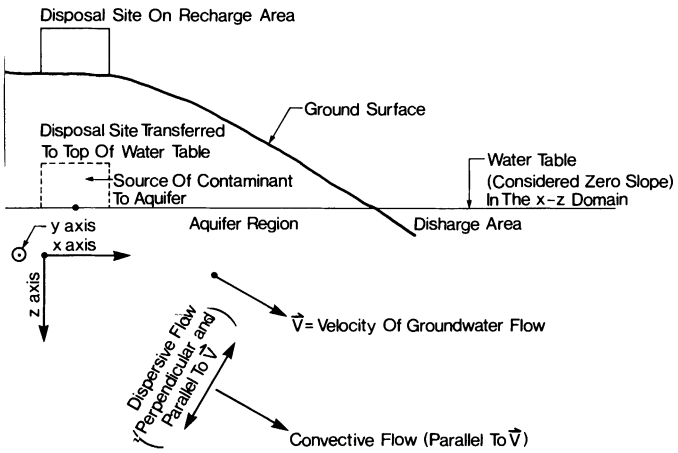

Fig. 1. The physical system of contaminant injection into and transport through an aquifer.

The Physical Problem

Consider the disposal site of length 2L and width 2L situated on a recharge area as shown in Fig. 1. Further, consider the disposal site as being responsible for the direct injection of contaminants into the horizontal (in the laboratory system) water table.A right-handed Cartesian coordinate system is established with the origin at the mid point of the disposal site with X-axis along the top surface of the aquifer, and Z-axis directed positively into the saturated zone. Let the groundwater flow velocity in the porous aquifer be $\bar{V}$. The convective contaminant flow will then be parallel to $\bar{V}$ while the dispersive contaminant flow may be parallel or perpendicular to $\bar{V}$. The velocity $\bar{V}$ will possess components V_x, V_y and V_z in the Cartesian coordinate system. An aquifer will be considered to be defined as isotropic if $V_x = V_y = V_z$. An aquifer in which the velocity ratios V_x/V_y and/or $V_x/V_z >> 1$ will be considered to be defined as highly anisotropic.

Theory

The mathematical model presented here follows the developments suggested by Hart et al. (1970), with suitable modifications to incorporate the effects of convective transport.

The material balance equation for dispersion, convection, and chemical reaction of material »*i*« at a concentration C_i and time t in a fluid flowing through a reactive porous media is given by

$$\frac{\partial C_i}{\partial t} + \bar{\nabla} \cdot \bar{J}_i = \pm R_i(C,t) \tag{1}$$

where

$\partial C_i / \partial t$ = Time rate of change of the fluid concentration of material »*i*«,

R_i = Rate of chemical reaction of »*i*« with the porous medium,

$$J_i = -D_i \bar{\nabla} C_i + \bar{V} C_i \tag{2}$$

= flux of contaminant concentration

where D_i is the dispersion coefficient (in units of length ^{2}/time) and $\bar{V}$ is the average groundwater velocity.

The first term of Eq. (2) defines the dispersive component of the flux and the second term defines the convective component.

Combining Eqs. (1) and (2) yields

$$\frac{\partial C_i}{\partial t} = \bar{\nabla} \cdot (D_i \bar{\nabla} C_i - \bar{V} C_i) \pm R_i(C,t) \tag{3}$$

Assuming the chemical reaction between the solution and solid phases to be an adsorptive reaction, and following Ogata (1964), the general form of R_i is taken to be

$$R_i = K_1(C - K_2 S) \tag{4}$$

where

S = concentration of solute in the solid phase

K_1 and K_2 = chemical reaction coefficients

Assuming K_2S to be much smaller than the concentration of fluid, Eq. (4) reduces to

$$R_i = K_1 C \text{ or } KC \tag{5}$$

describing an irreversible chemical raction (such as, for example, long-lived radioactive decay). By introducing Eq. (5) into Eq. (3), the two-dimensional mass transport equation in the horizontal (X-Y) domain becomes

$$\frac{\partial C}{\partial t} = D_x \frac{\partial^2 C}{\partial x^2} + D_y \frac{\partial^2 C}{\partial y^2} - V_x \frac{\partial C}{\partial x} - V_y \frac{\partial C}{\partial y} - KC \tag{6}$$

Consider the injected contaminant of concentration C to be defined as a unit step-function in both space and time. The boundary conditions within the X-Y domain then become

$$
\begin{array}{llll}
C = 1 & -L<X<L & -L<Y<L & 0<t<t_1 \\
C = 0 & -L<X<L & -L<Y<L & t_1<t<t_2 \\
C = 0 & -L<X<L & -L<Y<L & t=0 \\
C = 0 & x>L \text{ and } x<-L & & t=0 \\
C = 0 & y>L \text{ and } y<-L & & t=0
\end{array} \tag{7}
$$

Similarly, the mass transport equation and boundary conditions of the vertical (Z-X) domain are

$$
\frac{\partial C}{\partial t} = D_x \frac{\partial^2 C}{\partial x^2} + D_z \frac{\partial^2 C}{\partial z^2} - V_x \frac{\partial C}{\partial x} - V_z \frac{\partial C}{\partial z} - KC \tag{8}
$$

and

$$
\begin{array}{llll}
C = 1 & -L<X<L & Z\leq 0 & 0<t<t_1 \\
C = 0 & -L<X<L & Z\leq 0 & t_1<t<t_2 \\
C = 0 & -L<X<L & Z\leq 0 & t=0 \\
C = 0 & X>L \text{ and } X>-L & & t=0 \\
C = 0 & Z>0 & & t=0
\end{array} \tag{9}
$$

Physically, the contaminant injection is considered to progress through three phases. During the build-up phase ($0<t<t_1$) the contaminant concentration instantly and continuously assumes a normalized value of $C = 1$ at the source and this is reflected as a progressive build-up of contaminant within the aquifer. At $t = t_1$ a steady state phase is established within the aquifer and the flux of contaminant entering any infinitesimal volume of the saturated zone is equal to the flux leaving that volume. At this time $t = t_1$, the step-function source is turned off, and the contaminant concentration within the aquifer is allowed to dissipate (recovery phase) through convection and dispersion ($t_1 \geq t \geq t_2$).

The current work is further parameterized as follows:

a) distances in the X, Y, and Z directions are expressed in units of the half-length of the disposal site L;
b) the concentration of contaminants is expressed in terms of the ratio of total dissolved solids (TDS) in the saturated zone at time t to the recharge water concentration at time t=0;
c) following Bear (1972), the dispersion coefficients, D_x, D_y, and D_z, are taken to be proportional to the components of $\bar{V}$, viz. $D_x = \alpha V_x$; $D_y = \beta V_y$; $D_z = \gamma V_z$ where α, β, and γ are the dispersivities;
d) the water table aquifer rests on a horizontal impermeable base;
e) the hydrogeologic properties of the aquifer remain constant in both space and time;

f) internal forces, temperature gradients and osmotic pressure gradients are considered negligible;
g) time is reckoned in days;
h) the aquifer system is considered both prior and subsequent to the attainment of a steady-state condition.

Finite Difference Model

Analytical methods for the solution of the transport equation have been developed for relatively simple cases. Actual situations of groundwater flow systems possess a high degree of complexity, rendering complete agreement between theoretical predictions and field measurements very difficult. Numerous numerical methods (Stone et al. 1963; Shamir et al. 1967; Gardener et al. 1964; Pinder et al. 1970) have been developed during the past two decades. Marino (1974) has developed a finite difference integration approximation for the distribution of contaminants inside an adsorbing porous medium for the case of a one-dimensional flow field. In a similar manner, the current work utilizes both forward and central difference methods to solve Eqs. (6) and (8) and therefore describe the dispersion, convection, and chemical reaction of the contaminant within the aquifer in a duo two-dimensional manner, both prior and subsequent to the attainment of a steady-state condition.

Expressing integration in the time domain by means of the forward difference method yields

$$\left[\frac{\partial C}{\partial t}\right]^{k}_{i,j} = \frac{C^{k+1}_{i,j} - C^{k}_{i,j}}{\Delta t} \tag{10}$$

while expressing integration in the spatial domain by means of the central difference method yields

$$\left[\frac{\partial C}{\partial x}\right]^{k}_{i,j} \equiv \frac{C^{k}_{i+1,j} - C^{k}_{i-i,j}}{2(\Delta x)} \tag{11}$$

$$\left[\frac{\partial^2 C}{\partial x^2}\right]^{k}_{i,j} = \frac{C^{k}_{i-1,j} - 2C^{k}_{i,j} + C^{k}_{i+1,j}}{(\Delta x)^2} \tag{12}$$

$$\left[\frac{\partial C}{\partial z}\right]^{k}_{i,j} \equiv \frac{C^{k}_{i,j+1} - C^{k}_{i,j-1}}{2(\Delta z)} \tag{13}$$

and

$$\left[\frac{\partial^2 C}{\partial z^2}\right]^k_{i,j} = \frac{C^k_{1,j-1} - 2C^k_{i,j} + C^k_{i,j+1}}{(\Delta z)^2} \qquad (14)$$

where

$\Delta x, \Delta z, \Delta t$ = numerical increments of x, z, and t, respectively,
i,j,k = non-negative integers corresponding to x, z, and t, respectively

Substituting Eqs. (11) to (14) into Eqs. (6) and (8) will yield the governing finite integration approximations to the contaminant transport equations in the X-Y and Z-X domains, respectively.

The numerical solution for the horizontal *(X-Y)* domain thus becomes

$$\begin{aligned} C^{k+1}_{i,j} = {} & C^k_{i,j}(1 - 2A_x - 2A_y - m) + C^k_{i-1,j}(A_x + 0.5B_x) + \\ & C^k_{i+1,j}(A_x - 0.5B_x) + C^k_{i,j-1}(A_y + 0.5B_y) + \\ & C^k_{i,j+1}(A_y - 0.5B_y) \end{aligned} \qquad (15)$$

The numerical solution for the vertical *(Z-X)* domain thus becomes

$$\begin{aligned} C^{k+1}_{i,j} = {} & C^k_{i,j}(1 - 2A_x - 2A_z - m) + C^k_{i-1,j}(A_x + 0.5B_x) + \\ & C^k_{i+1,j}(A_x - 0.5B_x) + C^k_{i,j-1}(A_z + 0.5B_z) + \\ & C^k_{i,j+1}(A_z - 0.5B_z) \end{aligned} \qquad (16)$$

where the dimensionless parameters A_x, A_y, A_z, B_x, B_y, B_z, and m are given by

$$A_x = \frac{D_x \Delta t}{(\Delta x)^2} \; ; \quad A_y = \frac{D_y \Delta t}{(\Delta y)^2} \; ; \quad A_z = \frac{D_z \Delta t}{(\Delta z)^2}$$

$$B_x = \frac{V_x \Delta t}{\Delta x} \; ; \quad B_y = \frac{V_y \Delta t}{\Delta y} \; ; \quad B_z \equiv \frac{V_z \Delta t}{\Delta z}$$

$$m \equiv K \Delta t$$

The stability criteria (O'Brien et al. 1951; Smith 1965) for Eqs. (15) and (16) are

$$\left|\frac{D_x \Delta t}{(\Delta x)^2} + \frac{V_x \Delta t}{\Delta x}\right| + \left|\frac{D_z \Delta t}{(\Delta z)^2} + \frac{V_z \Delta t}{\Delta z}\right| \leq 1$$

and

$$K \Delta t \leq 1$$

To ensure against the possibility of numerical dispersions affecting the solutions of the finite difference equations, the criteria (Hirsh et al. 1974; Lam et al. 1976) on the Peclet numbers are taken as

$$P_{e_1} = \frac{V_x \Delta x}{D_x} \leq 2 \quad \text{and} \quad P_{e_2} = \frac{V_z \Delta z}{D_z} \leq 2$$

Effect of Velocity Ratios on Steady-State Attainment

Clearly, the time required for a point within an infinitesimal volume of the aquifer system to achieve a steady-state condition is dependent upon its spatial separation from the source and the relative values of the components of the groundwater flow velocity. In this work, a steady-state situation at a point is considered to be established at that value of t beyond which the computed concentration (from Eqs. (15) and (16) with a continuous constant injection concentration $C_i = 1$) does not change by more than 5%.

The principal direction of groundwater motion in an anisotropic horizontal unconfined aquifer is along the X-direction (defined as positive in the current system) and the higher the degree of anisotropy displayed by the aquifer, the higher will be the ratios V_x/V_y and/or V_x/V_z (a totally isotropic aquifer would be characterized by $V_x = V_y = V_z$).

Figs. 2 and 3 display the times (as determined from the solutions of Eqs. (15) and (16) necessary for the aquifer system of Fig. 1 to achieve the steady-state

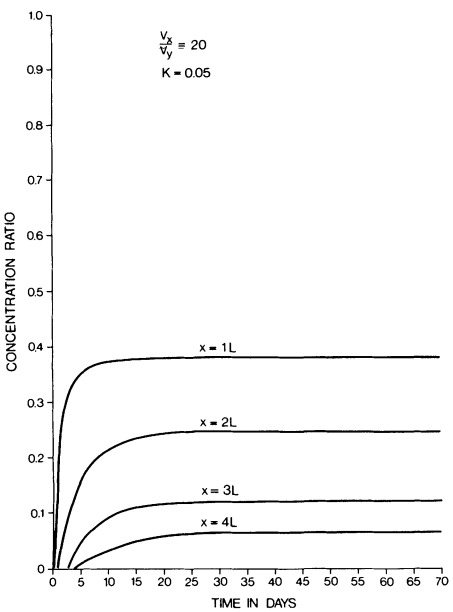

Fig. 2. Contaminant build-up stage at various stations along the water table (positive x-axis).

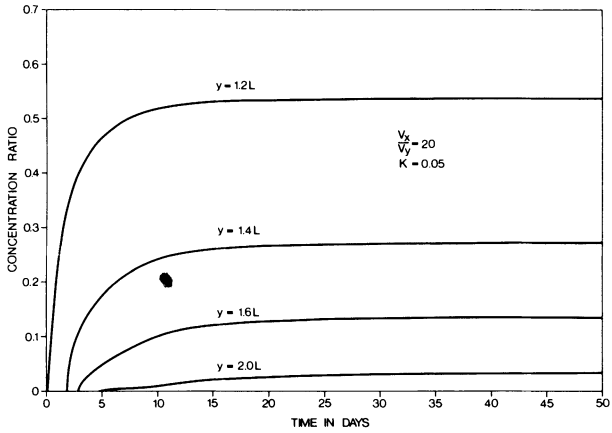

Fig. 3. Contaminant build-up stage at various stations along the water table (positive *y*-axis).

concentrations for a variety of distances (in terms of half-length L) from the origin and measured in the horizontal *(X-Y)* plane. The velocity ratio V_x/V_y is taken to be 20 (an anisotropy not unreasonable in terms of anticipated permeabilities for a large number of Canadian lakes and river basins) and the adsorption coefficient K is taken to be 0.05 during the build-up phase. Steady-state concentration conditions are then seen to be reached after 10, 15, and 20 days at distances of $1L$, $2L$, and $4L$, from the origin respectively, in the X-domain, and after 12, 15, 17, and

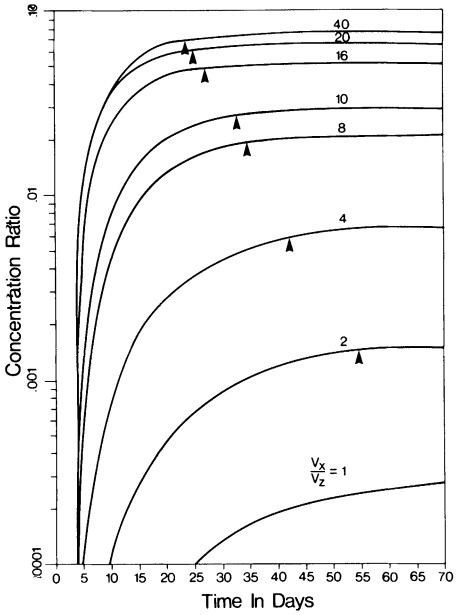

Fig. 4. The effect of principal velocity ratios on the build-up stage.

19, days at distances of 1.2L, 1.4L, 1.6L, and 2.0L from the origin, respectively, in the Y-domain.

In a similar manner, steady-state concentration attainment times may be determined for groundwater motion in the Z-X plane.

The effect of anisotropic groundwater flow on the rise time (i.e., time to attain a condition of steady-state flow) is shown in Fig. 4 for a variety of velocity ratios. The concentration of contaminant observed at a distance $X = 4L$ (and on the water table, i.e., $Z=0$) is plotted as a function of time for each considered velocity ratio V_x/V_z. It is clearly seen that as the velocity ratio increases, the steady-state condition is reached subsequent to considerably more rapid rise-times and the apparent steady-state concentration is dramatically increased.

Contaminant Concentration Profiles

Fig. 5 illustrates the steady-state solution (for continuous source injection) of Eq. (15) for the horizontal X-Y domain assuming $K = 0.05$ and $V_x/V_y = 20$. The salient features of the iso-concentration curves of Fig. 5 are:

a) Clearly, the contaminant concentration decreases in a quasi-exponential manner as distance from the source increases.
b) The contaminant is transported to shorter distances in the lateral (Y-axis) direction than in the downstream (X-axis) direction.
c) Distinct, albeit limited, contaminant transport is also apparent in the upstream (-X-axis) direction, the cause of which may be the consequence of molecular dispersion acting in opposition to the forcing velocity.

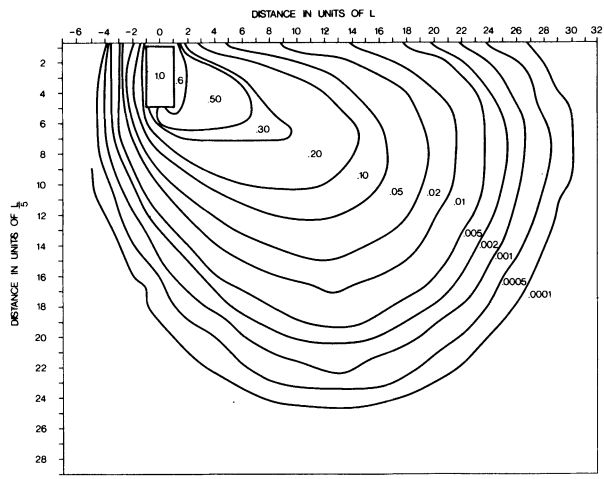

Fig. 5. Steady-state contaminant isoconcentration lines in the horizontal (x-y) domain.

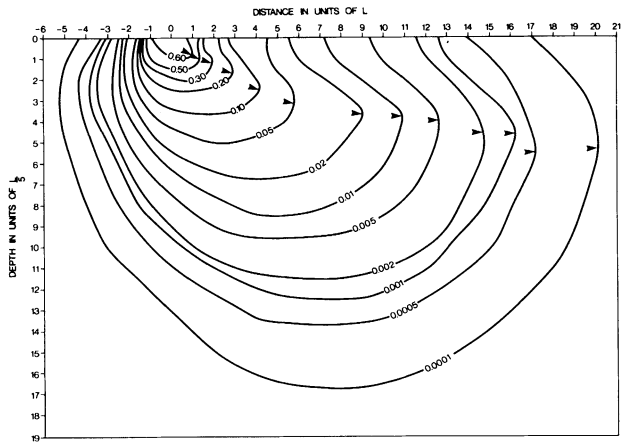

Fig. 6. Steady-state contaminant isoconcentration lines in the vertical (z-x) domain.

Similarly, Fig. 6 displays the steady-state iso-concentration profile for the Z-X domain as determined from a solution of Eq. (16). Once again V_x/V_z is taken as 20 and K is taken as 0.05. The salient features of the groundwater motion in the vertical domain are obvious counterparts of the features characterizing the groundwater motion in the horizontal domain, including the apparent molecular dispersion in the »backflow« negative X-direction.

The result of contaminant motion in the X-Y plain (subsequet to 50 days of continuous recharging at the source) is shown in Fig. 7. Herein are plotted the calculated concentrations as a function of distance along the X-axis for four representative distances along the Y-axis. The peak of contaminant concentration is

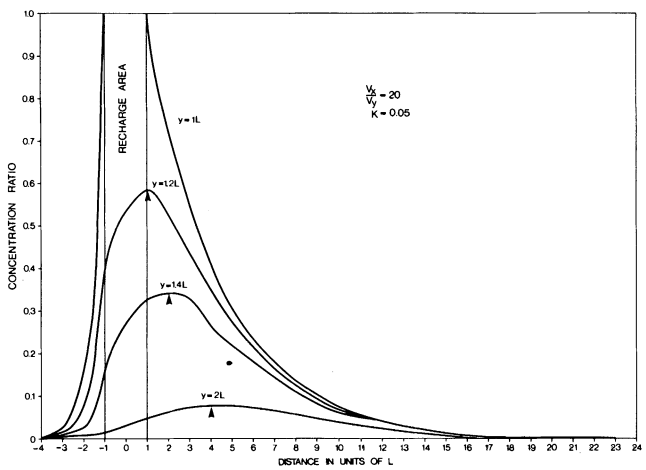

Fig. 7. Contaminant concentration profiles along the x-axis for various positions along the y-axis.

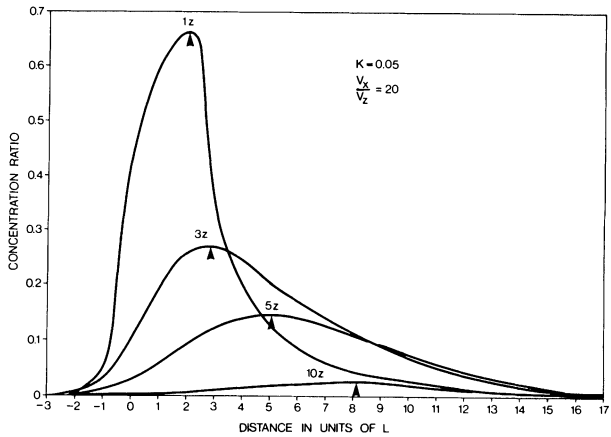

Fig. 8. Contaminant concentration profiles along the x-axis for various depths along the z-axis.

seen to have moved both laterally and downstream from the source, asymptotically reaching zero concentration at distances far removed from the recharge area. Similarly, the result of contaminant motion in the Z-X plane (subsequent to 50 days of continuous recharge) is shown in Fig. 8, and once again the two-dimensional migration of peak contamination concentration is clearly evident.

Steady-state concentration profiles for vertical sections at successively-increasing downstream distances from the source are shown in Fig. 9. Clearly evident is the reduction in peak concentration levels combined with a penetration to shallower depths beneath the water table. Once again, the contaminant concentration peak is seen to move along the resultant direction of groundwater flow.

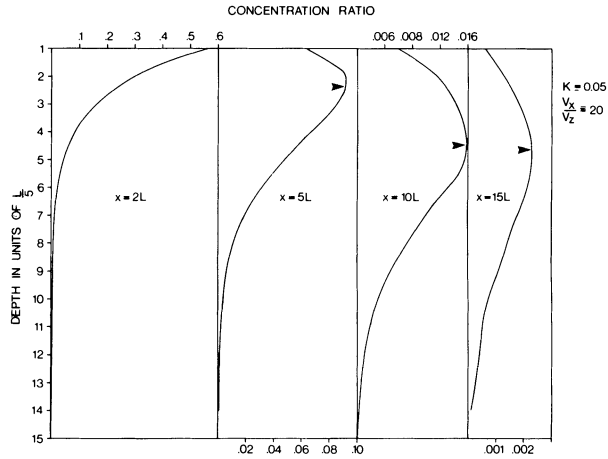

Fig. 9. Contaminant concentration profiles along the z-axis for various positions along the x-axis.

The Effect of Adsorption on Contaminant Concentration

In this work, the chemical reaction which results in the removal of contaminant from the fluid to the solid phase is considered to be a retarding effect due to the adsorption of contaminant on the porous medium. Mathematically, therefore, the porous medium acts as a sink. Fig. 10 illustrates the steady-state concentration profiles along the X-axis (for a velocity ratio $V_x/V_y = 20$ and subsequent to 50 days of continuous recharge) for different values of the adsorption coefficient K. It is evident that:

a) with increasing values of K, the peak contaminant concentration moves closer to the source;
b) with increasing values of K, less contamination is apparent at any point along the water table, including »backflow« concentrations upstream from the source; and
c) contaminant concentration becomes an increasingly more localized phenomenon with increasing K.

Similarly, Fig. 11 illustrates the effect of adsorption on the vertical propagation of injected contaminant. Once again, it is seen that an increase in K results in decreasing concentrations becoming more localized at shallower depths.

Effect of Velocity Ratios on Concentration Profiles

The influence of velocity ratios on steady-state contaminant transport along the principal flow direction (X-axis) and along the downward Y direction are illustrated in Figs. 12 and 13, respectively. In the vertical domain, increasing the velocity ratio results in an obvious more localized (albeit less intense) concentration of contaminant becoming apparent at shallower depths. In the horizontal domain (along the upmost surface boundary of the aquifer), it is seen that an isotropic aquifer (velocity ratio = 1) displays a Poisson-type concentration distribution which becomes increasingly more skewed in the principal-axis direction as the aquifer displays a higher order of anisotropy (i.e., velocity ratio increases) resulting in a very gradual migration of a reduced peak concentration to greater distances downstream from the source. It is evident, therefore, that an essentially isotropic aquifer will transport contaminant concentrations to deeper depths, while a sharply anisotropic aquifer will transport contaminant concentrations to much greater distances downstream. This duo two-dimensional contaminant transport dependence upon aquifer anisotropy is shown in Fig. 14. Herein are illustrated the steady-state 0.5% isoconcentration curves determined for several different velocity ratios. The extent of contaminant influence is seen to move to progressively shallower depths and larger downstream distances as the velocity ratio increases (i.e., as higher order anisotropic groundwater movement is encountered).

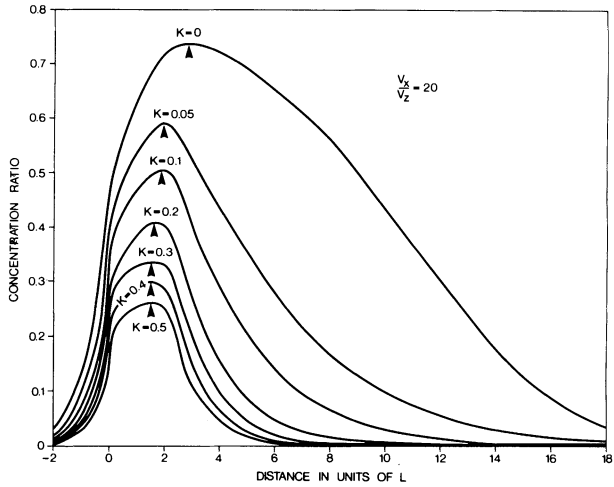

Fig. 10. Contaminant concentration profiles along the x-axis for various values of the adsorption coefficient K.

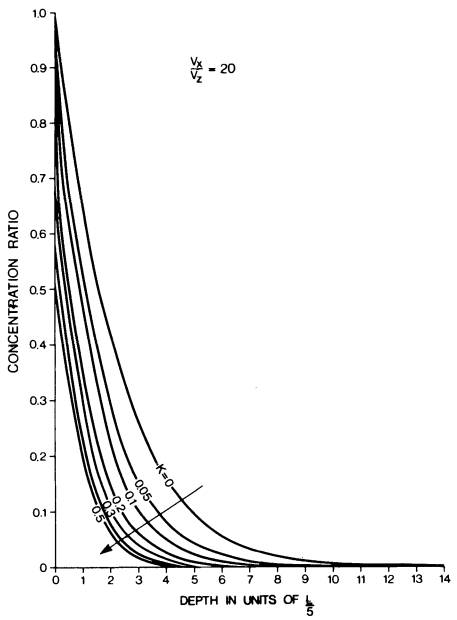

Fig. 11. Contaminant concentration profiles along the z-axis for various values of the adsorption coefficient K.

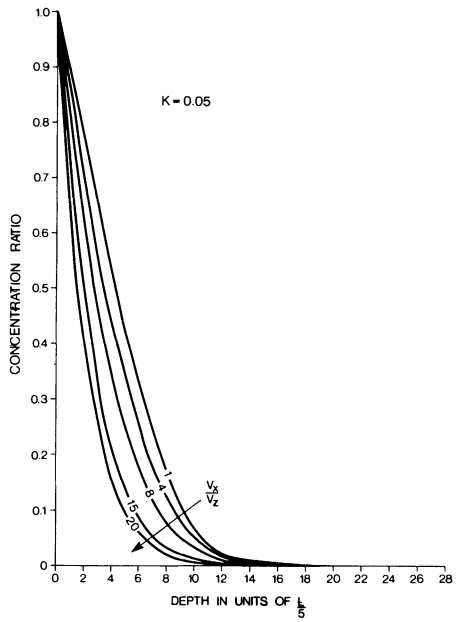

Fig. 12. Contaminant concentration profiles along the x-axis for various principal velocity ratios.

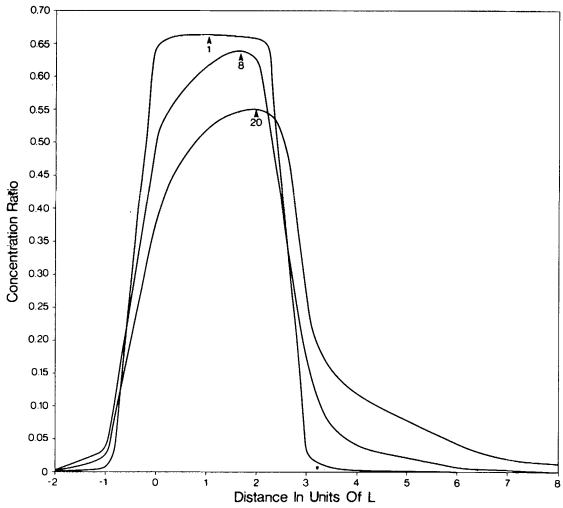

Fig. 13. Contaminant concentration profiles along the z-axis for various principal velocity ratios.

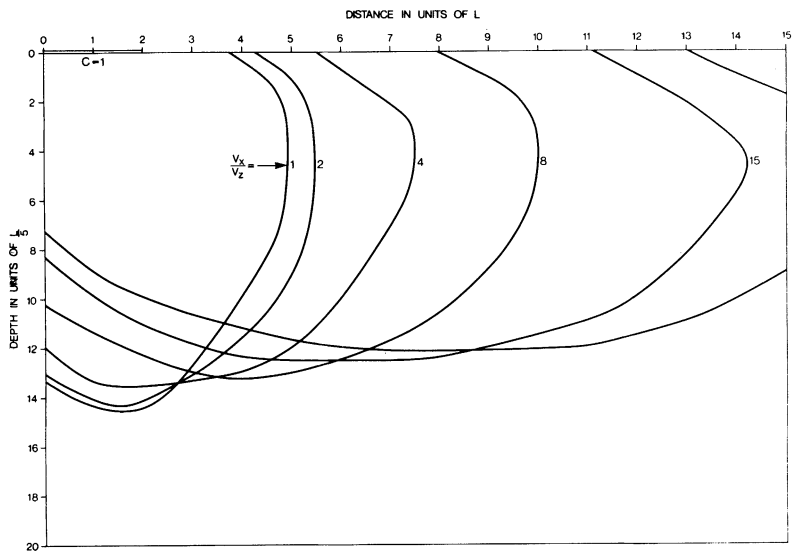

Fig. 14. A representative contaminant isoconcentration line in the z-x domain for various velocity ratios.

The Effect of Dispersitivity on Contaminant Profiles

The hydrodynamic dispersion coefficient D (for small Reynolds numbers) may be expressed (Bear 1972) as

$$D = D_m + \varepsilon |V|$$

where

D_m is the effective molecular diffusion coefficient of the porous medium under consideration.

ε is the dispersivity with X, Y, Z components of α, β and γ, respectively, and, V is the average pore water velocity.

In order to assess the effects of varying ε we assume that the molecular diffusion D_m may be represented by a constant value. For such a situation

$$D_x \sim V_x$$
$$D_y \sim V_y$$
$$D_z \sim V_z$$

Fig. 15 illustrates the build up of contaminant concentration in the subsurface system (at distance $X = 5L$ from the source) for two dissimilar velocity ratios (a near isotropic aquifer of $V_x/V_z = 2$ and a highly anisotropic aquifer of $V_x/V_z = 20$) for varying dispersivity ratios α/γ of 1, 5, 15, and 25. It is seen that the higher velocity ratio displays an independence of rise times with varying diffusivity ratios, while a distinct dependence upon diffusivity is displayed by the steady-state con-

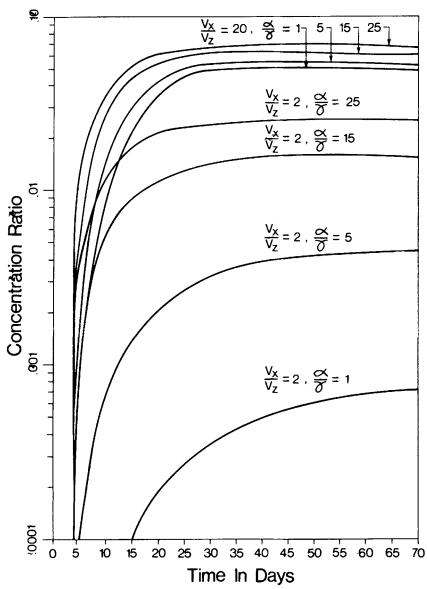

Fig. 15. Contaminant build-up stages of a near isotropic (V_x/V_z=2) and a highly anisotropic (V_x/V_x=20) aquifer for various dispersivity ratios α/γ.

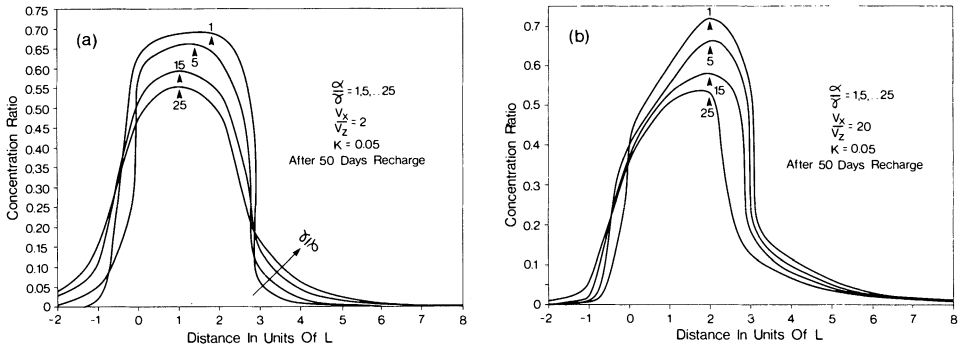

Fig. 16. Contaminant concentration profiles along the x-axis for various dispersivity ratios.
(a) near-isotropic aquifer
(b) highly anisotropic aquifer

centration values achieved by near-isotropic subsurface systems. The steady-state contaminant concentrations of highly anisotropic porous media are considerably less dependent upon dispersivity ratios. This clearly indicates that groundwater flow through highly anisotropic subsurface systems are largely under control of convective transport processes, while groundwater flow through subsurface systems approaching isotropy are largely dominated by hydrodynamic dispersive transport processes.

The spatial distribution of steady-state contamination (after 50 days of continuous recharge) along the water table (positive X-axis) is illustrated in Fig. 16. Fig. 16(b) considers an anisotropic aquifer defined by a high velocity ratio V_x/V_z = 20, while Fig. 16(a) considers a near-isotropic aquifer defined by a low velocity ratio V_x/V_z = 2. The profiles determined for dispersivity ratio α/γ = 1, 5, 15, and 25 are sketched in both figures for K = 0.05. For high velocity ratios it is seen that a) the peak contaminant concentration decreases with increasing dispersivity ratio , and b) the physical location of the peak contaminant concentration along the water table is essentially invariant. For low velocity ratios it is seen that a) the peak contaminant concentration also decreases with increasing dispersivity ratio, but b) the physical location of the peak contaminant concentration along the water table migrates farther downstream from the source as the dispersivity ratio decreases. As perhaps expected, a considerably more pronounced skewness is apparent in the X-axis contaminant distribution associated with anisotropic transport.

The spatial distribution of steady-state contamination (after 50 days of continuous recharge) along the Z-axis is illustrated in Fig. 17. Again, the anisotropic V_x/V_z = 20) condition is depicted in Fig. 17(b) and the near-isotropic V_x/V_z = 2) condition is depicted in Fig. 17(a). The profiles determined for dispersivity ratios α/γ = 1, 5, 15, and 25 are sketched for K = 0.05. Very slight differences are

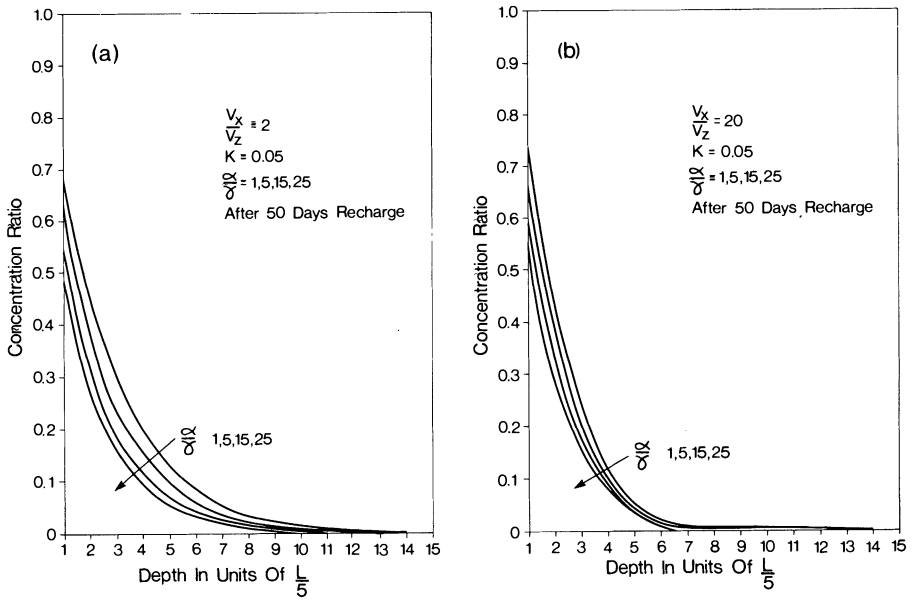

Fig. 17. Contaminant concentration profiles along the z-axis for various dispersivity ratios
(a) near-isotropic aquifer
(b) highly anisotropic aquifer

noticed between the anisotropic and isotropic situation. In both cases increasing the dispersivity ratios results in a more localized contaminant concentration being transported to shallower depths, although the effect of dispersion is slightly more significant for lower velocity ratios.

The Decay or Recovery Phase

Figs. 18 and 19 display the calculated recovery of the aquifer zone in the horizontal and vertical directions, respectively, subsequent to the termination of 10 days of continuous source injection. Once again the velocity ratio is taken to be 20 and K is taken to be 0.05. From the concentration profiles depicted in Fig. 18, it is seen that the recovery pattern along the downstream direction is one of an exponential decrease in peak concentration value coupled with an exponential migration of this peak concentration downstream.

The recovery pattern is considerably more complex in the vertical domain. Fig. 19 depicts the vertical concentration profiles calculated for stations located at distances of $3L$, $6L$, and $10L$ downstream from the source. The profiles have been determined for several days following termination of source injection at day 10.

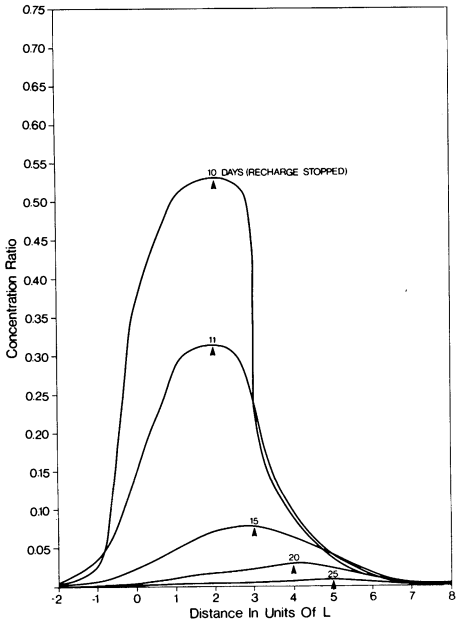

Fig. 18. Aquifer recovery stage contaminant concentration profile along the x-direction.

The dotted lines in Fig. 19 define the loci of the location in depth of the peak contaminant concentration. Close to the source (station at $X=3L$) a fairly rapid exponential (in time) collapse to pre-injection conditions is observed as the contaminant is transported downwards. For locations further downstream from the source (station at $X=6L$) the peak concentration continues to increase in magnitude and remain essentially at the steady-state depth before a downward propagation of contaminant accompanies an exponential evacuation of contaminant from the area. Such decay phase phenomena are even more evident at locations substantially removed from the source (station $X = 10L$) where clearly the presence of contaminant is readily apparent for more than two months subsequent to the termination of continuous injection.

Summary

A duo two-dimensional deterministic model which considers the dispersion, convection, and chemical adsorption processes of contaminant propagation in a porous medium has been developed and applied to a study of such contaminant motion in an anisotropic unconfined aquifer. Finite difference techniques have been applied to this model to consider the effects on contaminant transport of such parameters as degree of anisotropic groundwater flow (as indicated by principal velocity ratios), the adsorption coefficient, and the dispersivity ratios.

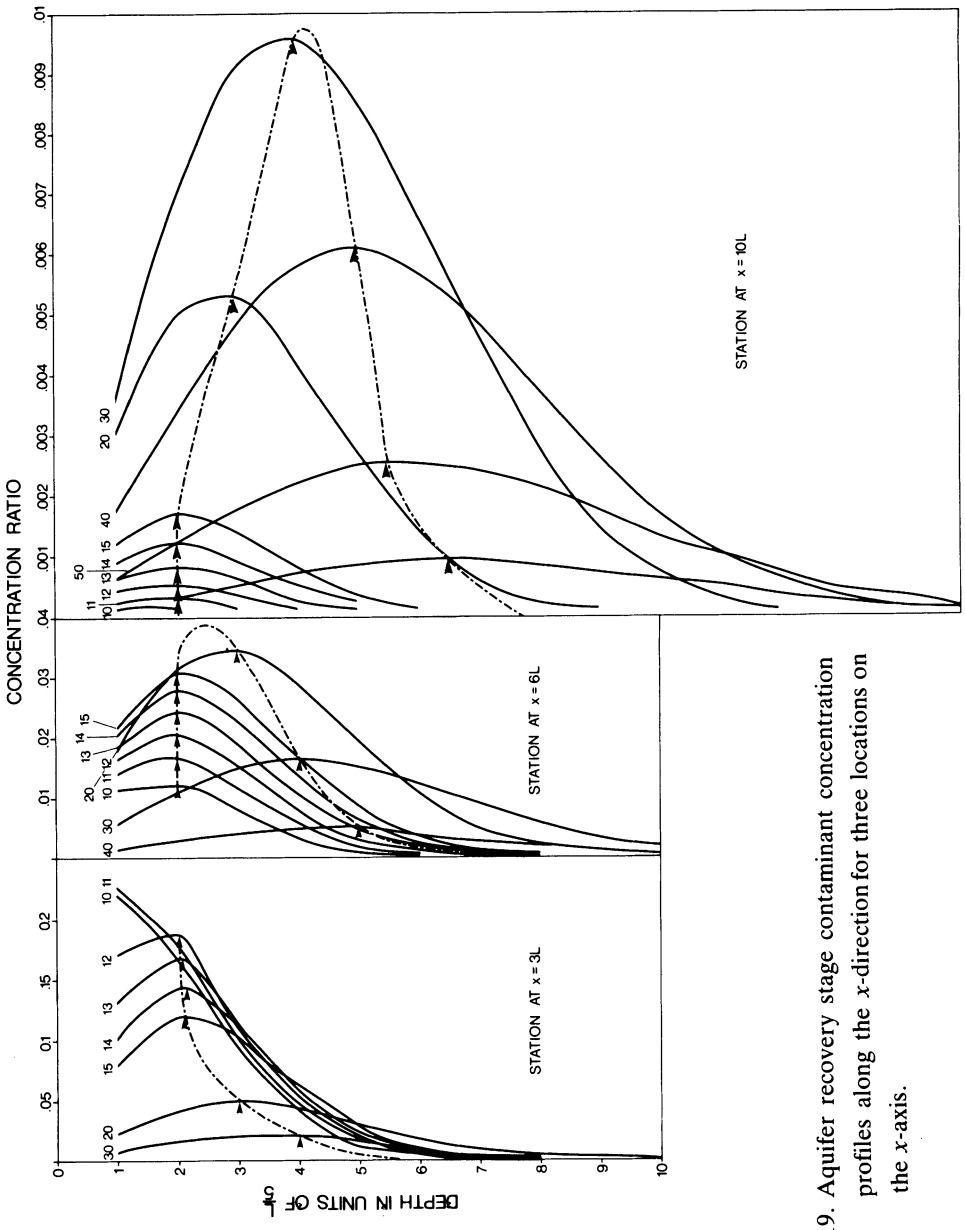

Fig. 19. Aquifer recovery stage contaminant concentration profiles along the x-direction for three locations on the x-axis.

The effect and range of influence of continuous contaminant injection into a rather simplistic aquifer has been considered here. The water table has been assumed horizontal, and the porous medium comprising the aquifer has been considered homogeneous enough to be defined by an average value of K which may be considered to be constant in both space and time. Current modelling work being performed at NWRI is being directed towards an evaluation of aquifers more closely resembling naturally found basin conditions, and results from these modelling efforts should be shortly forthcoming. Nevertheless, even on the basis of the simplified approach presented here, it is evident that such parameterization of groundwater flow motion in an anisotropic unconfined aquifer has immediate application to such issues and concerns as physical, chemical, and radioactive waste disposal and the long range transport of air pollutants through acidic precipitation.

Acknowledgements

The authors acknowledge, with thanks, their invaluable discussions with Drs. D.C.L. Lam and C.R. Murthy, and Messrs. J.E. Bruton and J.H. Jerome. Assistance of many kinds was provided by Miss L. Baskhar. Critical comments and suggestions were graciously provided by Prof. W. N. Stammers of the University of Guelph.

References

Banks, R.B., and Iqbal, A. (1964) Dispersion and adsorption in a porous media flow. *J. Hydraulic Div., Amer. Soc. Civil Eng., Vol. No. 90, No. HY5,* pp 13-31.

Bear, J. (1972) *Dynamics of fluids in porous media.* American Elsevier, New York, London, Amsterdam, 764 pp.

Bredehoeft, J.D., and Pinder, G.F. (1972) The application of the transport equations to a groundwater system. International Geological Congress, Montreal, Canada, Hydrogeology, Section II, pp 255-263.

Gardener, A.O., Peaceman, D.W., and Pozzi, Jr. A.L. (1964) Numerical calculation of multidimensional miscible displacement by the method of characteristics. *Jour. Soc. Petroleum Engrs., Vol. No. 4,* pp. 26-36.

Hart, H.E., Sugerman, D., and Shelupsky, D.I. (1970) Concentration equations for the diffusion of a reversibly reacting substance in gel-like media. *Bulletin of Mathematical Biophysics. Vol. No. 32,* pp 377-390.

Hirsh, R.S., and Rudy, D.H. (1974) The role of diagonal dominance and cell Reynolds number in implicit difference methods for fluid mechanics problems. *Jour. of Computational Physics. Vol. No. 16,* pp 304-310.

Kay, B.D., and Elrick, D.E. (1967) Adsorption and movement of lindane in soil. *Soil Science. Vol. No. 104,* pp 314-322.

Lam, D.C.L., and Simpson, R.B. (1976) Centered differencing and the Box Scheme for diffusion convection problems. *Jour. of Computational Physics. Vol. No. 22,* pp 486-500.

Lindstrom, F.T., and Bousma, L. (1973) A theory of the mass transfer of previously distributed chemicals in a water-saturated sorbing medium: III. Exact solution for first order kinetic sorbtion. *Soil Science, Vol. No. 115,* pp 5-10.

Lapidus, L., and Amundson, N.R. (1952) Mathematics of adsorption in beds. VI. The effect of longitudinal diffusion in ion exchange and chromatographic columns. *Jour. Phy. Chem. Vol. No. 56,* pp 984-988.

Marino, M.A. (1974) Numerical and analytical solutions of dispersion in a finite, adsorbing porous medium. Water Resources Bulletin. Vol. No. 10, pp 81-90.

O'Brien, G.G. *et al.* (1951) A study of the numerical solution of partial differential mathematics. *Jour. of Mathematics and Physics, Vol. No. 29,* pp 223-251.

Ogata, A. (1964) Mathematics of dispersion with linear adsorption isotherm. U.S. Geol. Survey Proj. paper, 411-G, 11 pp.

Shamir, V.Y., and Harleman, D.R.F. (1967) Numerical solutions for dispersion in porous mediums. *Water Resources Research, Vol. No. 3,* pp 557-581.

Smith, G.O. (1965) *Numerical solution of partial differential equations.* Oxford University Press, New York and London. 179 pp.

Stone, H.L., and Brian, P.L.T. (1963) Numerical solution of convective transport problems. *Jour. A. Inst. Chem. Eng. Vol. No. 9,* pp 681-688.

van Genuchten, M. Th., Davidson, J.M., and Wierenga, P.J. (1974) An evaluation of kinetic and equilibrium equations for prediction of pesticide movement through porous media. *Soil Sci. Soc. Am. Proc. 38;* 29-35.

Received: 8 May, 1980

Address:
Aquatic Physics and Systems Division,
National Water Research Institute,
Canada Centre for Inland Waters,
867 Lakeshore Road,
P.O. Box 5050,
Burlington, Ontario, Canada,
L7R 4A6.